

**ISCI, Volume 13**

**Supplemental Information**

**Spatiotemporally Controlled Myosin**

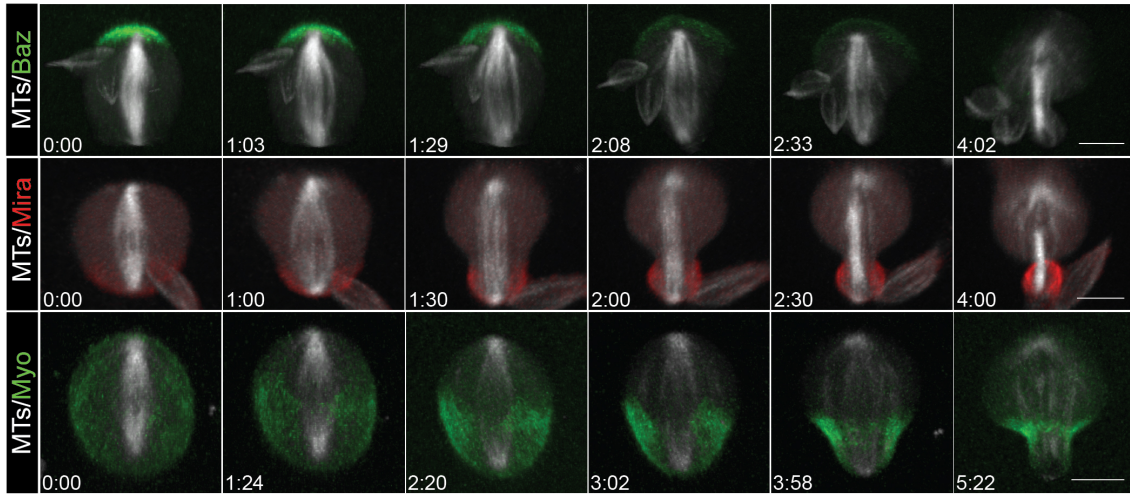
**Relocalization and Internal Pressure**

**Generate Sibling Cell Size Asymmetry**

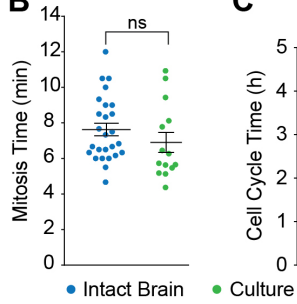
**Tri Thanh Pham, Arnaud Monnard, Jonne Helenius, Erik Lund, Nicole Lee, Daniel J. Müller, and Clemens Cabernard**

# Supplemental Figures

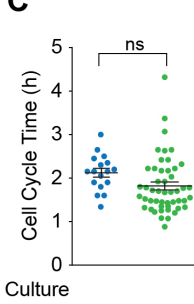
**A**



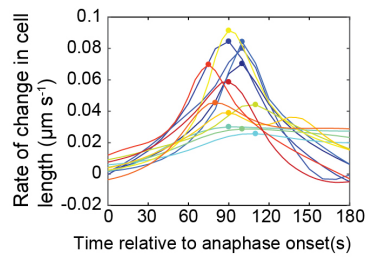
**B**



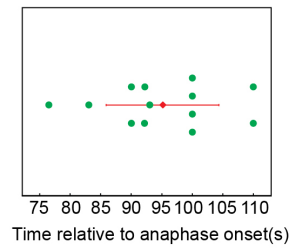
**C**



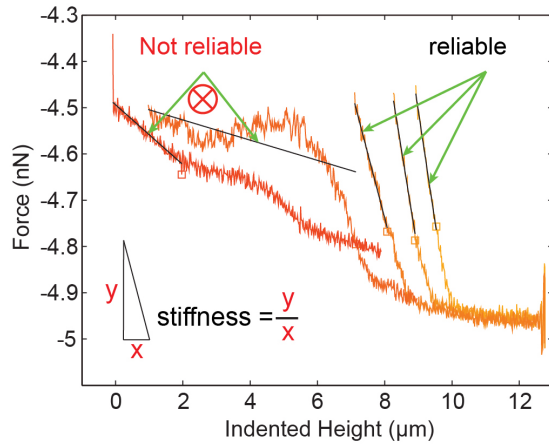
**D**



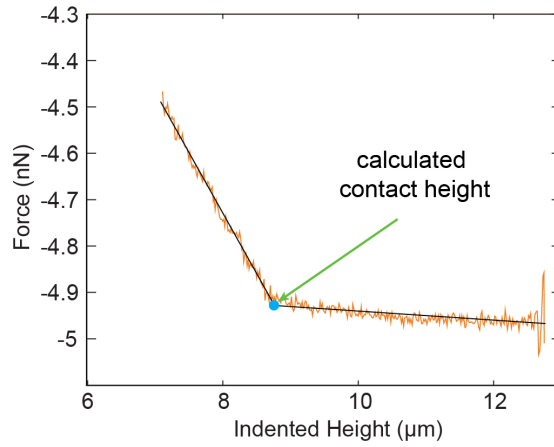
**E**



**F**



**G**



**H**

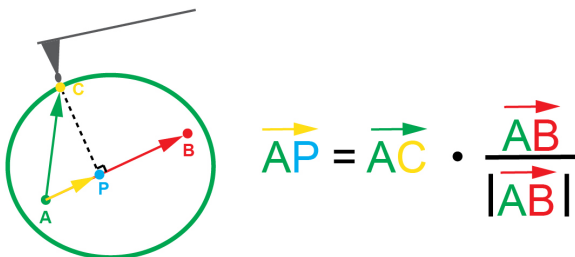


**Figure S1. Cultured neuroblasts can be used to measure biophysical parameters, Related to Figure 1.**

**(A)** Representative image sequence of a cultured wild type neuroblast expressing the apical polarity marker Baz::GFP (green; top row), the basal cell fate determinant Miranda (red; middle row) and the cell cortex marker Sqh::GFP (green; bottom row). All shown cells co-express the mitotic spindle marker pUAST-Cherry::Jupiter (white). Scatter plots showing **(B)** mitosis time and **(C)** the cell cycle time for cultured larval neuroblasts (green dots; n = 14 and 49) compared to larval neuroblasts in intact brains (blue dots; n = 26 and 17). **(D)** Graph showing the rate of change in cell length for several wild type neuroblasts in an intact brain (n=13). **(E)** Scatter plot showing the time when the peak rate of change in cell length occurs relative to anaphase onset. **(F)** Representative graph showing the raw AFM data for force versus indented height. Reliable cortical stiffness was extracted from the force vs indented height curve that fit well to a linear line for a portion of the raw data. **(G)** Representative graph showing how contact height was determined. **(H)** Schematic diagram showing how an AFM contact point can be projected onto the spindle axis to be sorted into regions for statistical averaging. Scale bar: 5  $\mu\text{m}$ . Asterisk denote statistical significance, derived from unpaired t-tests: \*,  $p \leq 0.05$ , \*\*,  $p \leq 0.01$ , \*\*\*,  $p \leq 0.001$ , \*\*\*\*;  $P \leq 0.0001$ , n.s.; not significant.

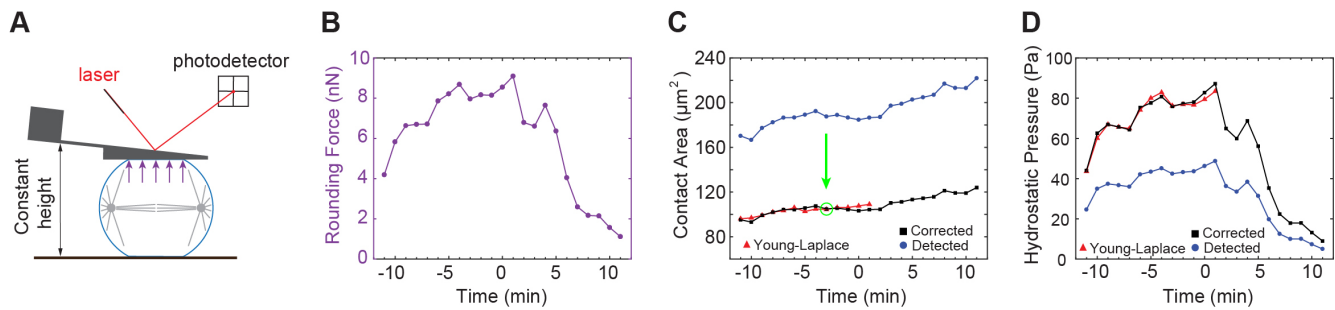


**Figure S2. Rounding force increases during mitosis, peaking right after anaphase onset, Related to Figure 2.**

**(A)** Schematic representation of a parallel plate assay (constant height assay) used to measure hydrostatic pressure throughout mitosis. **(B)** Rounding force detected by AFM throughout mitosis for a representative cell. The time axis is relative to anaphase onset (0 min). **(C)** Contact area was determined by two independent methods. (1) Theoretical contact area (red) calculated using the uniform tension model is very accurate, however it is only valid as long as cells are spherical. (2) Contact area detected by the total cell area that are in contact with the AFM wedge using fluorescent signal (blue). This method can be used at all cell cycle stages, but it tends to overestimate the contact area due to the point spread function of the imaging system. A correction factor (obtained at time point indicated by the green arrow) was applied to contact area measurements based on Young-Laplace calculations for spherical cells. **(D)** Hydrostatic pressure for the chosen representative cell was plotted per Young-Laplace (red), the detected contact area (blue) and the corrected contact area (black).



**Figure S3. Myosin relocalization is essential for cortical expansion, Related to Figure 3&4.**

Representative image sequences and kymographs obtained along the apical-basal axis and the furrow region of third instar neuroblasts expressing Sqh::GFP for **(A, B)** wild type, **(C, D)** *pins* mutant, **(E, F)** pUAST-CAAX::vhhGFP expressing wild type neuroblasts, **(G, H)** colcemid treated *rod* mutant neuroblasts, **(I, J)** EIPA treated wild type neuroblasts and **(K, L)** EIPA treated *pins* mutant neuroblasts and Y-27632 treated wild type neuroblasts resulting in complete **(M, N)** or partial **(O, P)** Rok inhibition. Change in expansion length for both apical (green) and basal (red) cortex before and after furrow constriction (furrow diameter reduction) for partial Y-27632 treated wild type neuroblasts (n=14) and colcemid treated *rod* mutant neuroblasts (n=12) are shown in **(Q)** and **(R)**, respectively. **(S, T)** Scatter plot showing the onset of apical expansion (green), onset of furrow constriction (blue) and onset of basal expansion (red) for colcemid treated *rod* mutant neuroblasts (n=12) and Y-27632 treated wild type neuroblasts (n=14), respectively. **(U)** Scatter plot showing the sibling cell size ratio for Y-27632 treated wild type neuroblasts (n=14) and colcemid treated *rod* mutant neuroblasts (n=12), compared to wild type neuroblasts (n=19). Kymographs obtained along the apical-basal axis showing the dynamic change in furrow positioning for **(V)** wild type neuroblasts and **(W)** EIPA treated wild type neuroblasts. **(X)** Scatter plot showing the furrow shift during mitosis for wild type neuroblasts (n=19) and EIPA treated wild type neuroblasts (n=11). Time: seconds (s). Scale bar: 5  $\mu$ m. Yellow time scale bar in kymographs: 2 min.

## Transparent Methods

### CONTACT FOR REAGENT AND RESOURCE SHARING

Further information and requests for resources and reagents should be directed to and will be fulfilled by the Lead Contact, Clemens Cabernard ([ccabern@uw.edu](mailto:ccabern@uw.edu)).

### EXPERIMENTAL MODEL AND SUBJECT DETAILS

#### Fly strains and genetics

The following mutant alleles were used: *pins*<sup>P89</sup> (Yu et al. 2000), *pins*<sup>P62</sup> (Yu et al. 2000), *rod*<sup>H4.8</sup> (Basto et al. 2000), *sqh*<sup>AX3</sup> (Jordan & Karess 1997).

Transgenes and fluorescent markers: *worGal4*, *pUAST-Cherry::Jupiter* (Cabernard & Doe 2009), *worGal4*, *pUAST-Cherry::Jupiter*, *Sqh::GFP* (Cabernard et al. 2010), *worGal4*, *pUAST-Cherry::Jupiter*, *pUAST-Mira::GFP* (Cabernard & Doe 2009), *Baz::GFP* (Buszczak et al. 2007), *Sqh::GFP* (Royou et al. 2002), *pUAST-Cnn::EGFP* (Megraw et al. 2002), *pUAST-pH::EGFP* (Bloomington stock center), *pUAST-attB-Caax::VhhGFP4* (this work), *pUAST-attB-PhyB::mcherry::CAAX* (this work).

#### Generation of transgenic lines

**pUAST-attB-CAAX::VhhGFP4:** The coding sequence of CAAX has been synthesized as oligonucleotides. VhhGFP4 (Saerens et al., 2005) was amplified by PCR (forward primer: AGGGAATTGGGAATTCCGCCACCATGGATCAAGTCCAACCTGGTG; reverse primer: TCTTCTTTTACGCGTGCTGGAGACGGTGACCTG) and cloned into the pUAST-attB vector using In-Fusion technology (Takara, Clontech). The resulting construct was injected into attP flies for targeted insertion on the third chromosome (VK00020, BestGene).

**pUAST-attB-PhyB::mcherry::CAAX:** The coding sequence of PhyB::mcherry::CAAX (Buckley et al., 2016) was amplified by PCR (Forward primer: GGGAATTGGGAATTC CGCCACCATGGTATCAGGTG;

Reverse primer: ACAAAGATCCTCTAGATTACATGAT AACACACTTGGTTTTTG) and cloned into the pUAST-attB vector using In-Fusion technology (Takara, Clontech). The resulting construct was injected into attP flies for targeted insertion on the third chromosome (VK00033, BestGene).

## METHOD DETAILS

### Colcemid, Y-27632 and EIPA experiments

For Y-27632 and colcemid and experiments, we used *worGal4, pUAST-Cherry::Jupiter, Sqh::GFP; pUAST-PhyB::mcherry::CAAX* and *worGal4, pUAST-Cherry::Jupiter, Sqh::GFP; rod<sup>H4.8</sup>*, respectively. For EIPA (ethylisopropylamiloride) experiments, we used *pins<sup>P89</sup>, pins<sup>P62</sup>* and *worGal4, pUAST-Cherry::Jupiter, Sqh::GFP*. Dissected brains were incubated with Y-27632 (LC Labs) in live imaging medium at a final concentration of 62.5  $\mu\text{g mL}^{-1}$ , with colcemid (Sigma) at a final concentration of 25  $\mu\text{g mL}^{-1}$ , or with EIPA (Sigma) at a final concentration of 150  $\mu\text{M}$ . Live imaging was acquired ~ 30 min after drugs addition. Complete spindle depolymerization was seen at the start of imaging for colcemid addition. Significant reduction of *Sqh::EGFP* on the neuroblast cortex was seen ~ 30 minutes after Y-27632 addition. Slight reduction in diameter of metaphase neuroblast was also observed ~ 30 minutes after EIPA addition.

### Live cell imaging

Third instar larvae were used for all live cell imaging experiments. Live cell imaging was performed as described previously (Doe 2013) with the following minor modifications: S2 Media (Invitrogen) was supplemented with 10% HyClone Bovine Growth Serum (BGS, Thermo Scientific SH3054102). The larval brains were dissected in the supplemented S2 media and transferred into a  $\mu$ -slide angiogenesis (ibidi). Live samples were imaged with an Andor revolution spinning disc confocal system, consisting of a Yokogawa CSU-X1 spinning disk unit and two Andor iXon3 DU-897-BV EMCCD cameras. A 60X/1.4NA oil immersion objective mounted on a Nikon Eclipse Ti microscope was used for most



images. Live imaging voxels sizes are 0.22 X 0.22 X 1 $\mu$ m (60x/1.4NA spinning disc).

*sqh<sup>AX3</sup>*; *worGal4*, *pUAST-Cherry::Jupiter*, *Sqh::GFP*; *pUAST-CAAX::VhhGFP4* larvae were kept at 18 °C and then incubated at 29°C up to 6h prior to imaging.

### **Image processing and measurements**

Live cell imaging data was processed using Imaris x64 7.5.4 and ImageJ. Andor IQ2 files were converted into Imaris files using a custom-made Matlab code. Average intensity projections were generated in ImageJ. All Kymographs obtained from a line drawn from the apical to the basal cortex were generated with a 5-pixel wide. All Kymographs obtained from the furrow site were generated with a 9-pixel wide line. The intensity values at the apical, basal and furrow site, as well as in the cytoplasm were extracted using a custom-made Matlab code (Cortex position and intensity extract from kymograph analysis.m). For the intensity plots, the cortical intensities were normalized against the cytoplasmic values. The intensity at the cleavage furrow was obtained from an average value between the left and the right furrow cortex values. The curvature analysis was performed in ImageJ, using a custom made Matlab code (Cortex intensity and curvature extract from drawn boundary.m). Cortical intensities along the cell boundary were obtained from an average intensity of three pixels located perpendicular to the cell boundary.

Figures were assembled using Adobe Illustrator CS6 and all quantifications were performed in Matlab and Microsoft Excel.

### **Primary larval neuroblast culture procedure**

Primary neuroblast cultures were prepared as previously reported (Berger et al. 2012). In brief, wild type brains were dissected in Chan and Gehring's medium and incubated with Collagenase Type I (Sigma) and Papain (Sigma) at 30° C for 30 min at a final concentration of 1mg/mL. The brains were gently washed twice with 400  $\mu$ L of supplemented Schneider's medium. The brains were then placed in a 1.5

mL tube with 200  $\mu\text{L}$  of supplemented Schneider's medium and homogenized using a 200  $\mu\text{L}$  pipette tip by pipetting several times until the solution looked homogenous.

### **AFM measurements**

All stiffness measurements were performed using a Nanowizard II JPK AFM (JPK Instruments, Germany), coupled with an inverted optical microscope (Zeiss Axiovert 200, Germany). All experiments were performed in solution using intermittent contact. In order to measure cortical stiffness, isolated wild type neuroblasts expressing Sqh::EGFP and Cnn::EGFP were plated on a cover-glass bottom dish (FluoroDish, WPI, INC., Sarasota, FL, USA). The cover-glass bottom disc was coated with 10  $\mu\text{g mL}^{-1}$  of Concanavalin A to anchor the cell to the glass surface and prevent slippage when pressing the cell with the AFM tip. The sample was placed on the AFM stage mounted on top of the optical microscope. A Plan Apochromat 63X/1.4NA oil immersion objective was used together with the Zeiss AxioCam MRm monochrome digital camera to sequentially acquire fluorescent images with cortical stiffness measurements. Live imaging voxels sizes are 0.0993 X 0.0993 X 1  $\mu\text{m}$  (63x/1.4NA). High aspect ratio bead tipped cantilevers with a nominal spring constant of 0.2  $\text{N m}^{-1}$  and a tip height in the range of 10-15  $\mu\text{m}$  with a spherical 300 nm radius (B300\_CONTR, Nanoandmore, Germany) were employed. A force-volume line scan consisting of 30 equally spaced measurement points along a 20  $\mu\text{m}$  line was used to probe local cortical stiffness with a maximal applied force of 0.6 nN. The extension velocity and the extension length were set at 20  $\mu\text{m s}^{-1}$  and 8  $\mu\text{m}$ , respectively. Each image stack and the subsequent line scan took approximately 30 s to complete. Unreliable AFM measurements, visible in the force curves, were excluded from the analysis (Figure S1F,G).

To determine the neuroblast's mitotic stage we used Cnn::GFP to measure the distance between centrosomes at all measured time points and plotted the cell elongation rates, which usually peaked at around 90 s after anaphase onset. This provided a measurement for determining the mitotic stage with  $\sim 30$  s accuracy (Figure S1D,E).

## QUANTIFICATION AND STATISTICAL ANALYSIS

### Curvature analysis

To determine the local curvature along the cell cortex, a line was manually drawn in ImageJ from the apical to the basal cortex on the mid-plane. Local cortical curvature  $K$  can be determined via the following formula:  $K = \frac{f''(x)}{(1+f'^2(x))^{3/2}}$ , where  $x$  and  $f(x)$  are the horizontal and vertical position of the drawn cortex, respectively. The first and second derivatives ( $f'(x)$  and  $f''(x)$ ) of the curve were calculated numerically using second order difference methods. Custom-written Matlab codes (Cortex intensity and curvature extract from drawn boundary.m) were used to determine curvature values for all points on the curve.

### Kymograph quantification

Cell mid-planes were first generated using the Oblique Slicer tool in Imaris (Bitplane) and the entire image volume was then resliced along the direction of this plane for all time points. Using ImageJ, an average intensity projection was generated from three selected planes closest to the mid-plane. This procedure was done for all acquired time points. Kymographs were then generated by drawing a five pixel wide straight line from the apical to the basal cortex for all time points. To determine cortical intensity signal from a kymograph, a spline curve was drawn along the cortex on the kymograph and the XY coordinates of this curve were exported to a text file. Custom made Matlab codes (Cortex position and intensity extract from kymograph analysis.m) were written to extract the exact XY coordinates of the drawn curve from the text file without any repetitive time points by using a standard interpolation method. Intensity signal of the drawn curve was calculated from the grayscale kymograph image using an average intensity of the three pixels, closest to the curve.

## **Onset of expansion/constriction quantifications**

The position of the apical, basal and furrow site cortices were traced by drawing a spline curve along each of these boundaries using the Kymographs generated earlier. The onset of expansion was chosen at the time point when the cortex expands to 3% of the cell metaphase radius (i.e. radius at 30 s before anaphase onset was used in this case). The onset of constriction was set in a similar manner. This 3% change in radius value was chosen because it is equivalent to a one pixel change on the image obtained from the 60X objective, which can also be detected by eye.

## **Cortical stiffness quantifications**

Cortical stiffness is obtained from the slope of the linear part of the force-depth curve. Data with a force range from 60% to 100% of the maximal force was used to fit a linear regression curve (Figure S1). To determine the reliability of the cortical stiffness extracted from the fitted line, the mean square error of the fit was used. The extracted cortical stiffness is classified as a reliable measurement when the mean square error of the fit is lower than the mean peak-peak fluctuation of the system, which is  $\sim 0.015$  nN. Only reliable measurements were used to determine statistical average for each local region along the cell.

To determine the location of the AFM measurement points relative to the cell spindle-axis, precise location of the cell centrosomes and the contact point where the AFM tip touches the cell's surface is required. The contact height for any measurement point was determined from the point along the force vs indentation height curve that fit the curve best with two linear lines. The position of each centrosome was obtained from the xyz location of a spot placed at the highest intensity signal of the centrosomal marker Cnn::EGFP. The xy position of all AFM measurement points were determined by recording the first and the last position of the AFM tip. The centrosome height and the AFM contact height were synchronized using the cell mid-plane at metaphase as the reference height. The location of the cortical stiffness measurement relative to the spindle axis between the two centrosomes was determined using vector projections. At any cell cycle stage, the distance between the two centrosomes was binned into

20 equally distributed regions and reliable cortical stiffness measurements were accumulated for statistical average.

### **Pressure quantifications**

Isolated wild type neuroblasts expressing pUAST-Cherry::Jupiter and pUAST-PH::EGFP were plated on a WPI glass bottom disc without any coating. The sample was placed on a JPK Cellhesion 200 stage which was mounted on top of a Zeiss confocal microscope (LSM 700). A custom-made flat PDMS wedge tip was held constantly at 5  $\mu\text{m}$  above the glass bottom surface above the neuroblast. As the neuroblast enters mitosis, it rounds up and exerts a force on the wedge AFM tip, which can be detected by the photodetector. A Plan Apochromat 63X/1.4NA oil immersion objective was used to simultaneously image the neuroblast every minute while recording the exerted force. Hydrostatic pressure can be determined by taking the ratio of the detected forces and the area that was in contact with the wedge (Stewart et al. 2013).

### **Correlation plots**

To determine the correlation between any two quantities of interest which were acquired independently, a normalized root-mean-square deviation method (Maiorov & Crippen 1994) was used, hereby defined as the deviation coefficient. To obtain the deviation coefficient for all regions at a particular time point, the two curves were first normalized before the absolute difference was calculated. The deviation coefficients for all time point throughout mitosis was accumulated and normalized to their maximum value (NRMSD). A low deviation coefficient indicates a high correlation.

### **Definition of statistical tests, sample number, sample collection, replicates.**

Analyses were performed with MATLAB and Graphpad Prism. For each experiment, the data was collected from at least 3 independent experiments. For each independent experiment, at least 5 larvae

were dissected. Statistical significance was determined using two-sample equal or unequal variance  $t$ -tests. Significance was indicated as following: \*,  $p < 0.05$ , \*\*,  $p < 0.01$ , \*\*\*,  $p < 0.001$ , \*\*\*\*,  $p < 0.0001$ . ns; not significant.

## DATA AND SOFTWARE AVAILABILITY

### MATLAB codes

**AndorIQ to Imaris merge autosave.m:** This code first imports the primary channel of Andor IQ raw data into Imaris and then adds the slave channel of Andor IQ raw data into Imaris as a second channel. The file was automatically saved once both channels were successfully loaded into Imaris.

**AFM reliability analysis.m:** This code imports the raw data recorded from the AFM experiments and extracts cortical stiffness and contact height. The reliability of cortical stiffness was characterized by how well the linear region of the force curve fit to a straight-line compared to the mean peak-to-peak fluctuation of the system.

**AFM region statistics.m:** This code reads the coordinates of the centrosomes as well as the calculated cortical stiffness and contact height from the text files to determine the position of the measurement points relative to the spindle axis. The cell mid-plane at metaphase was used as a reference height for both the centrosomes and the AFM measurement points. The data was binned into 20 equal regions along the spindle axis and accumulated from all measured cells to determine statistical averages.

**Cortex position and intensity extract from kymograph analysis.m:** This code reads the Kymograph .tiff image and the coordinate .txt files which recorded the position of the apical and basal cortex, and the cytoplasm for each time point on the kymograph. Since ImageJ automatically interpolated the

position coordinates from a drawn line, the coordinate .txt file contains more time points than present. This code filters out the repeated time points and calculates the average intensity at each position for all time points.

**Cortex intensity and curvature extract from drawn boundary.m:** This code reads the coordinates of the cell cortex boundary from the text files to determine the curvature and Myosin intensity at each pixel position on the cell cortex along the apical-basal division axis.

**Deviation coefficient analysis.m:** This code calculates the root-mean-square difference between any two quantities and normalizes the outcome to the absolute maximum value, generating the deviation coefficient for all regions and time points provided.

**Rounding force extract at each imaging time point.m:** This code extracts the rounding force at recorded time point to calculate the hydrostatic pressure.

**Pressure calculation using theoretical contact area.m:** This code detects the cell boundary and calculates the area inside the cell for each slice to determine the mid-plane slice with the largest cross section. Theoretical contact area was calculated using the best fitted radius for the mid-plane slice and the cell height under the AFM cantilever. Hydrostatic pressure was determined by taking the ratio of rounding force to the contact area.

**Pressure calculation using detected contact area.m:** This code reads the coordinate.txt file which contains the position of the outer boundary of the contact surface where the cell is in contact with the

AFM wedge. Hydrostatic pressure was determined by calculating the ratio between the rounding force and the detected contact area.

**Pressure calculation using correction factor.m:** This code calculates the ratio between the detected contact area and the theoretical contact area at a cell cycle stage when the cell mid-plane boundary fits the circle best. This ratio was used as a correction factor and applied to all the detected contact areas. The resulting product is the corrected contact area, which was used to determine the corrected hydrostatic pressure for all time points throughout mitosis.



## KEY RESOURCES TABLE

REAGENT or RESOURCE	SOURCE	IDENTIFIER
Biological Samples		
Larval brain tissues from wild type and mutant <i>Drosophila melanogaster</i> strains	This study	N/A
Chemicals, Peptides, and Recombinant Proteins		
Bovine Growth Serum	Thermo Scientific	Cat# SH3054102
Schneider's Insect Medium	Sigma-Aldrich	Cat# S0146
Colcemid (MT inhibitor)	Sigma-Aldrich	Cat# D7385
Rho kinase inhibitor Y-27632	LClabs	Cat# Y-5301
5-(N-Ethyl-N-isopropyl)amiloride (EIPA)	Sigma-Aldrich	Cat# A3085
Collagenase Type I	Sigma-Aldrich	Cat# C0130
Papain	Sigma-Aldrich	Cat# P4762
Chan and Gehring's medium	(Chan & Gehring 1971)	
Experimental Models: Organisms/strains		
<i>D. melanogaster. pins</i> <sup>P89</sup>	(Yu et al. 2000)	FBal0104444
<i>D. melanogaster. pins</i> <sup>P62</sup>	(Yu et al. 2000)	FBal0104445
<i>D. melanogaster. rod</i> <sup>H4.8</sup>	(Basto et al. 2000)	FBal0014638
<i>D. melanogaster. Sqh</i> <sup>AX3</sup>	(Jordan & Karess 1997)	FBal0035707
<i>D. melanogaster. worGal4, UAS-Cherry::Jupiter</i>	(Cabernard & Doe 2009)	FBtp0040573
<i>D. melanogaster. worGal4, UAS-Cherry::Jupiter, Sqh::GFP</i>	(Cabernard et al. 2010)	FBtp0040573
<i>D. melanogaster. Baz::GFP</i>	(Buszczak et al. 2007)	
<i>D. melanogaster. worGal4, UAS-Cherry::Jupiter; Mira::GFP</i>	(Cabernard & Doe 2009)	FBtp0041413
<i>D. melanogaster. Sqh::GFP</i>	(Martin et al. 2009)	FBF0151365
<i>D. melanogaster. UAS-Cnn::EGFP</i>	(Megraw et al. 2002)	FBF0152123
<i>D. melanogaster. UAS-pH::EGFP</i>	Bloomington	BDSC:39693
<i>D. melanogaster. pUAST-attP-PhyB::mCherry::CAAX</i>	This paper	
<i>D. melanogaster. pUAST-attP-CAAX::VhhGFP4</i>	This paper	
Oligonucleotides		
Forward primer for <i>pUAST-attP-CAAX::VhhGFP4</i> AGGGAATTGGGAATTCCGCCACCATGGATCAA GTCCAACCTGGTG	This paper	
Reverse primer for <i>pUAST-attP-CAAX::VhhGFP4</i> TCTTCTTTTTACGCGTGCTGGAGACGGTGACCT G	This paper	

Forward primer for <i>pUAST-attP-PhyB::mCherry::CAAX</i> GGGAATTGGGAATTCCGCCACCATGGTATCAG GTG	This paper	
Reverse primer for <i>pUAST-attP-PhyB::mCherry::CAAX</i> ACAAAGATCCTCTAGATTACATGATAACACACTT GGTTTTTG	This paper	
Recombinant DNA		
pUAST-attB-CAAX::VhhGFP4	This paper	
pUAST-attB-PhyB::mCherry::CAAX	This paper	
Software and Algorithms		
ImageJ	N/A	<a href="https://imagej.nih.gov/ij/">https://imagej.nih.gov/ij/</a>
Imaris 7.6.4	Bitplane	<a href="http://www.bitplane.com/imaris">http://www.bitplane.com/imaris</a>
MATLAB	Mathworks	<a href="https://www.mathworks.com">https://www.mathworks.com</a>
Prism	GraphPad	<a href="https://www.graphpad.com">https://www.graphpad.com</a>
Matlab code to calculate curvature values	This paper	
Matlab code to calculate deviation coefficients	This paper	
Matlab code to extract rounding forces	This paper	
Matlab code to calculate theoretical pressure	This paper	
Matlab code to calculate detected pressure	This paper	
Matlab code to corrected pressure	This paper	
Matlab code to convert raw imaging data files into Imaris (Bitplane) file format	This paper	

## Supplemental References

- Basto, R., Gomes, R. & Karess, R.E., 2000. Rough deal and Zw10 are required for the metaphase checkpoint in *Drosophila*. *Nature cell biology*, 2(12), pp.939–943.
- Berger, C. et al., 2012. FACS Purification and Transcriptome Analysis of *Drosophila* Neural Stem Cells Reveals a Role for Klumpfuss in Self-Renewal. *Cell reports*, 2(2), pp.407–418.
- Buszczak, M. et al., 2007. The carnegie protein trap library: a versatile tool for *Drosophila* developmental studies. *Genetics*, 175(3), pp.1505–1531.
- Cabernard, C. & Doe, C.Q., 2009. Apical/basal spindle orientation is required for neuroblast homeostasis and neuronal differentiation in *Drosophila*. *Developmental cell*, 17(1), pp.134–141.
- Cabernard, C., Prehoda, K.E. & Doe, C.Q., 2010. A spindle-independent cleavage furrow positioning pathway. *Nature*, 467(7311), pp.91–94.
- Chan, L.N. & Gehring, W., 1971. Determination of blastoderm cells in *Drosophila melanogaster*. *Proceedings of the National Academy of Sciences*, 68(9), pp.2217–2221.
- Doe, C.Q., 2013. Live imaging of neuroblast lineages within intact larval brains in *Drosophila*. *Cold Spring Harbor Protocols*, 2013(10), pp.970–977.
- Jordan, P. & Karess, R., 1997. Myosin light chain-activating phosphorylation sites are required for oogenesis in *Drosophila*. *The Journal of cell biology*, 139(7), pp.1805–1819.
- Maierov, V.N. & Crippen, G.M., 1994. Significance of root-mean-square deviation in comparing three-dimensional structures of globular proteins. *Journal of molecular biology*, 235(2), pp.625–634.
- Martin, A.C., Kaschube, M. & Wieschaus, E.F., 2009. Pulsed contractions of an actin-myosin network drive apical constriction. *Nature*, 457(7228), pp.495–499.
- Megraw, T.L. et al., 2002. The centrosome is a dynamic structure that ejects PCM flares. *Journal of cell science*, 115(Pt 23), pp.4707–4718.
- Royou, A., Sullivan, W. & Karess, R., 2002. Cortical recruitment of nonmuscle myosin II in early syncytial *Drosophila* embryos: its role in nuclear axial expansion and its regulation by Cdc2 activity. *The Journal of cell biology*, 158(1), pp.127–137.
- Stewart, M.P. et al., 2013. Wedged AFM-cantilevers for parallel plate cell mechanics. *Methods*, 60(2), pp.186–194.
- Yu, F. et al., 2000. Analysis of partner of inscuteable, a Novel Player of *Drosophila* Asymmetric Divisions, Reveals Two Distinct Steps in Inscuteable Apical Localization. *Cell*, 100(4), pp.399–409.